Leadership in Sustainable Infrastructure

Leadership en Infrastructures Durables

Vancouver, Canada

May 31 – June 3, 2017/ *Mai 31 – Juin 3, 2017*

ENGINEERED GRADED MATERIALS: VIBRATION OF DOUBLY-CURVED GRADED NANO-PANELS

Yazdani Sarvestani, H.[1], Akbarzadeh, A.H.[1,3], Mirabolghasemi, A.[1], Rankohi, S.[2]

[1] AM3L Laboratory, Department of Bioresource Engineering, McGill University, Montreal, Quebec H9X 3V9, Canada

[2] Canam Group, Montreal J4B 5X9, Canada

[3] hamid.akbarzadeh@mcgill.ca

ABSTRACT: Functionally graded materials (FGMs) as a type of engineered advanced materials are composed of the mixture of two or multiple materials or phases in a fashion that overall multiphysical properties gradually changes throughout the medium. Conventional plate and shell models based on the classical continuum theories, however, cannot capture the size effects occurring in nano/microstructure of FGMs due to the lack of material length scale in the formulation of classical continuum mechanics. As a result, plate and shell models based on the size-dependent continuum theories, such as couple-stress theory, have been recently revisited. In present paper, a size-dependent modified couple-stress model is developed for moderately-thick doubly-curved panels based on the first-order shear deformation theory. The non-classical model incorporates the material length scale parameter, which incorporates the size effect in the mechanical behavior. In specific, we investigate the free vibration of FGM doubly-curved nano-panels for alternative boundary conditions. The material properties of the FGM panel vary through the thickness direction, effective properties which are estimated through a multiscale homogenization technique. The governing equations are first derived by a variational formulation using Hamilton's principle and are solved afterwards using the numerical Galerkin method. Numerical results are finally presented to study the effects of the material length scale parameter and material compositions on the vibration behavior of FG doubly-curved nano-panels.

1 INTRODUCTIONS

Continuum mechanics theories based on the classical elasticity are not capable of simulating accurately the mechanical behavior of micro- and nano-structures. The culprit is the lack of length scale parameter in the formulation of deformation mechanism. In order to consider the scale effects, size-dependent continuum theories have been introduced as alternatives to classical continuum mechanics. Mindlin and Tiersten (1962), and Koiter (1964) developed couple stress theory with one length scale parameter, and Eringen (1972) presented a non-local elasticity model including two material length scales. Since measuring material length scales is a cumbersome task, requiring detailed multi-scale simulation from macro to micro and atomistic levels, many researchers have performed size-dependent analysis involving only one material length scale. For instance, Yang et al. (2002) proposed a modified couple stress theory where the couple stress tensor is symmetric and only one internal material length scale is involved in addition to Lamé's constants. The modified couple stress theory has been applied to study structural behavior of size-dependent micro- or nano-plates and shells. For instance, Park and Gao (2006) developed size-dependent Euler-Bernoulli beam and Ma et al. (2008) developed a size-dependent Timoshenko beam model on the basis of modified couple stress theory proposed by Yang et al. (2002). Afterwards, size-dependent Euler-

Bernoulli and Timoshenko beam models have been used to simulate structural behavior of micro-tubules (Kong et al. 2008), and micro-tubes conveying fluid (Wang 2010). In addition, plate and shell theories have been used along with the couple stress theory for analyzing microstructure-dependent materials and structures. For example, Tsiatas (2009) performed static analysis of micro-plates by introducing a microstructure-dependent model based on the classical plate theory. Later on, Hadjesfandiari and Dargush (2011) developed fundamental solutions for two- and three-dimensional linear isotropic size-dependent couple stress elasticity. Modified couple stress theory has been further developed to analyze advanced graded materials like FG micro-beams (Asghari et al. 2011) and FG micro-plates (Reddy et al. 2012).

In this paper, we establish a mathematical framework based on the modified couple stress theory and FSDT to study free and forced vibration analyses of size-dependent FG doubly-curved panels. While most of the papers in the literature on the structural response of FGMs have employed the approximate rule of mixture (micromechanical models) to obtain effective material properties (Akbarzadeh et al. 2014), herein we also implement a standard mechanics homogenization technique to accurately predict effective multi-physics properties of FGMs for a wide range of volume fractions of matrix for two simplified shapes of inclusion. Numerical results confirm the significance of implementing an accurate numerical homogenization technique for predicting overall properties of FGMs.

2 DISPLACEMENT FIELD IN SIZE-DEPENDENT FG DOUBLY-CURVED PANELS

A schematic representation of a size-dependent doubly-curved panel made of FGMs with constant principal curvatures is shown in Fig. 1. The curvilinear length, curvilinear width, and thickness of a size-dependent FG doubly-curved panel are represented by a, b, and h, respectively. The FG panels are presented in an orthogonal curvilinear coordinate system (x, y, z). The radii of principal curvatures of the middle surface are R_x and R_y overlapped along the coordinate axes. Consistent with the assumptions of a moderately-thick shell theory, the displacement field follows (Tornabene et al. 2013):

$$[1a] \qquad u(x,y,z,t) = \left(1+\frac{z}{R_x}\right)u_0(x,y,t) + z\varphi_x(x,y,t)$$

$$[1b] \qquad v(x,y,z,t) = \left(1+\frac{z}{R_x}\right)v_0(x,y,t) + z\varphi_y(x,y,t)$$

$$[1c] \qquad w(x,y,z,t) = w_0(x,y,t)$$

where u_0, v_0, and w_0 are the displacement components of points lying on the middle surface (z=0) of the doubly-curved panel, along meridian, circumferential and normal directions, respectively. Time variable is represented by t, while normal-to-mid-surface rotations are represented by φ_x, and φ_y. The general strain-displacement relations for a 3D solid shell in the coordinate system (x, y, z) are (Kiani et al. 2012):

$$[2] \qquad \varepsilon_{xx} = \frac{\partial u_0}{\partial x} + \frac{w_0}{R_x} + z\frac{\partial \varphi_x}{\partial x}, \qquad \gamma_{yz} = \frac{\partial w_0}{\partial y} - \frac{v_0}{R_y} + \varphi_y,$$

$$\varepsilon_{yy} = \frac{\partial v_0}{\partial y} + \frac{w_0}{R_y} + z\frac{\partial \varphi_y}{\partial y}, \qquad \gamma_{xz} = \frac{\partial w_0}{\partial x} - \frac{u_0}{R_x} + \varphi_x,$$

$$\gamma_{xy} = (1+zc_0)\frac{\partial u_0}{\partial y} + (1-zc_0)\frac{\partial v_0}{\partial x} + z\frac{\partial \varphi_x}{\partial y} + z\frac{\partial \varphi_y}{\partial x}$$

where ε_{ij} and γ_{ij} are normal and shear strain components, respectively. Besides, $c_0 = \frac{1}{2}(\frac{1}{R_x} - \frac{1}{R_y})$ is Sanders shell theory characteristic adopted here to account for zero-strain condition for rigid body motion.

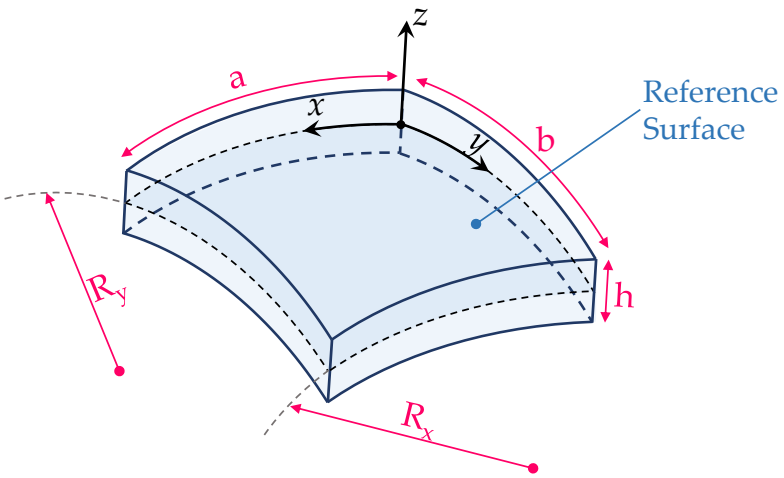

Figure 1: Coordinate system for a size-dependent FG doubly-curved panel.

As seen in Fig. 1, the doubly-curved formulations provided in this paper can reduce to a wide range of panels with constant curvatures, e.g. circular cylindrical shell for $R_y = \infty$, spherical panel for $R_x = R_y$, and saddle panel for $R_x = -R_y$ (see Fig. 1).

3 EQUATIONS OF MOTION OF SIZE-DEPENDENT FG DOUBLY-CURVED PANELS

Equations of motion for an FG doubly-curved panel are obtained using the principle of virtual displacements:

$$[3] \qquad \int_{t_1}^{t_2} \left(\delta U + \delta V - \delta K\right) dt = 0$$

where δU, δV, and δK are the virtual strain energy, virtual work done by external forces, and virtual kinetic energy, respectively. Based on modified couple stress theory, the equations of motion are developed. According to the modified couple stress theory, the virtual strain energy δU can be written as:

$$[4] \qquad \delta U = \int_V \left(\sigma_{ij}\delta\varepsilon_{ij} + m_{ij}\delta\chi_{ij}\right) dV$$

where Einstein summation convention is adopted. Here, σ_{ij}, ε_{ij}, m_{ij}, and χ_{ij} are the components of the Cauchy stress tensor, strain tensor, the deviatoric part of the couple stress tensor, and curvature tensor, respectively; it should be noted that m_{ij}, and χ_{ij} are symmetric. The total virtual kinetic energy δK can be expressed as (Kiani et al. 2012):

$$[5] \qquad \delta K = \int_{-h/2}^{h/2}\int_A \rho\left[\left(1+\frac{z}{R_x}\right)\dot{u} + z\dot{\varphi}_x\right]\left[\left(1+\frac{z}{R_x}\right)\delta\dot{u} + z\delta\dot{\varphi}_x\right] dA dz + \int_{-h/2}^{h/2}\int_A \rho\left[\left(1+\frac{z}{R_y}\right)\dot{v} + z\dot{\varphi}_y\right]\left[\left(1+\frac{z}{R_y}\right)\delta\dot{v} + z\delta\dot{\varphi}_y\right] dA dz$$
$$+ \int_{-h/2}^{h/2}\int_A \rho\dot{w}\delta\dot{w} dA dz$$

where ρ represents the panel density. The three-dimensional stress-strain relations for heterogeneous isotropic linear elastic materials used in this paper are written as follows (Reddy 2004):

$$[6] \qquad \begin{Bmatrix}\sigma_{xx}\\ \sigma_{yy}\\ \tau_{yz}\\ \tau_{xz}\\ \tau_{xy}\end{Bmatrix} = \begin{bmatrix} \frac{E(z)}{1-\nu^2(z)} & \frac{E(z)\nu(z)}{1-\nu^2(z)} & 0 & 0 & 0 \\ \frac{E(z)\nu(z)}{1-\nu^2(z)} & \frac{E(z)}{1-\nu^2(z)} & 0 & 0 & 0 \\ 0 & 0 & G(z) & 0 & 0 \\ 0 & 0 & 0 & G(z) & 0 \\ 0 & 0 & 0 & 0 & G(z) \end{bmatrix} \begin{Bmatrix}\varepsilon_{xx}\\ \varepsilon_{yy}\\ \gamma_{yz}\\ \gamma_{xz}\\ \gamma_{xy}\end{Bmatrix}, \qquad \text{and} \qquad m_{ij} = \frac{E(z)}{1+\nu(z)} l^2(z)\chi_{ij}$$

where E, G, υ, and l are Young's modulus, shear modulus, Poisson's ratio, and material length scale, respectively. In this research, we consider size-dependent two-phase FG doubly-curved panels. The FGMs are modeled here as a two-phase (inclusion and matrix) composite materials in which the composition of phases varies continuously

in the form of power-law (P-FGM) through the thickness of the doubly-curved nano-panel. The volume fraction of matrix varies as:

$$[7] \qquad V_f = V_{ft} + \left(V_{fb} - V_{ft}\right)\left(\frac{h-2z}{2h}\right)^p$$

where V_{ft} , and V_{fb} are the volume fraction of matrix at the top ($z = h/2$) and the bottom ($z = -h/2$) of FG panels, respectively; p and h stand for the power-law index and the thickness of the doubly-curved panel. The effective mechanical properties of FG doubly-curved panels will be obtained by a standard mechanics homogenization technique in Section 5 for each volume fraction of FGMs for two different shapes of inclusion. By substituting Eqs. (6) into Eq. (3) and, carrying out the necessary integrations, and employing the fundamental lemma of calculus of variations, we can develop the system of equations of motion for vibration analysis of size-dependent FG doubly-curved panels:

$$[8a] \qquad \delta u_0: \quad -N_{xx,x} - N_{xy,y} - c_0 M_{xy,y} - \frac{1}{2R_x}\left(2Q_{xz} + Y_{yy,y} + Y_{xy,x}\right) + \frac{1}{2}\left(c_0 Y_{zz,y} - Y_{yz,yy} - Y_{xz,xy}\right)$$
$$+ \frac{1}{4R_x}\left(\frac{1}{R_x} + \frac{1}{R_y}\right)Y_{yz} = -\left(I_1 + \frac{2}{R_x} I_2\right)\ddot{u}_0 - \left(I_2 + \frac{1}{R_x} I_3\right)\ddot{\varphi}_x$$

$$[8b] \qquad \delta v_0: \quad -N_{yy,y} - N_{xy,x} + c_0 M_{xy,y} - \frac{1}{2R_y}\left(2Q_{yz} - Y_{xx,x} - Y_{xy,y}\right) + \frac{1}{2}\left(c_0 Y_{zz,x} + Y_{xz,xx} + Y_{yz,xy}\right)$$
$$- \frac{1}{4R_y}\left(\frac{1}{R_x} + \frac{1}{R_y}\right)Y_{xz} = -\left(I_1 + \frac{2}{R_y} I_2\right)\ddot{v}_0 - \left(I_2 + \frac{1}{R_y} I_3\right)\ddot{\varphi}_y$$

$$[8c] \qquad \delta w_0: \quad \frac{1}{R_x} N_{xx} + \frac{1}{R_y} N_{yy} - Q_{xz,x} - Q_{yz,y} + \frac{1}{2}\left(Y_{xx,xy} - Y_{yy,xy} + Y_{xy,xy} - Y_{xy,xx}\right) + \frac{1}{4}\left(\frac{1}{R_x} + \frac{1}{R_y}\right)\left(Y_{yz,x} - Y_{xz,y}\right) = -I_1 \ddot{w}_0$$

$$[8d] \qquad \delta\varphi_x: \quad -M_{xx,x} - M_{xy,y} + Q_{xz} - \frac{1}{2}\left(Y_{yy,y} - Y_{zz,y} + Y_{xy,x} + T_{yz,yy} + T_{yz,xy}\right) + \frac{1}{4}\left(\frac{1}{R_x} + \frac{1}{R_y}\right)Y_{yz} = -\left(I_2 + \frac{1}{R_x} I_3\right)\ddot{u}_0 - I_3\ddot{\varphi}_x$$

$$[8e] \qquad \delta\varphi_y: \quad -M_{yy,y} - M_{xy,x} + Q_{yz} + \frac{1}{2}\left(Y_{xx,x} - Y_{zz,x} + Y_{xy,x} + T_{yz,xx} + T_{yz,xy}\right) - \frac{1}{4}\left(\frac{1}{R_x} + \frac{1}{R_y}\right)Y_{xz} = -\left(I_2 + \frac{1}{R_y} I_3\right)\ddot{v}_0 - I_3\ddot{\varphi}_y$$

where the classical and non-classical forces and moments are written as follows:

$$[9] \qquad \left(N_{xx}, N_{yy}, N_{xy}\right) = \int_{-h/2}^{h/2} \left(\sigma_{xx}, \sigma_{yy}, \tau_{xy}\right) dz \qquad \left(M_{xx}, M_{yy}, M_{xy}\right) = \int_{-h/2}^{h/2} \left(\sigma_{xx}, \sigma_{yy}, \tau_{xy}\right) z dz$$
$$\left(Q_{xz}, Q_{yz}\right) = k_s \int_{-h/2}^{h/2} \left(\tau_{xz}, \tau_{yz}\right) z dz \qquad \left(Y_{ij}, T_{yz}\right) = \int_{-h/2}^{h/2} \left(m_{ij}, m_{yz} z\right) dz$$

where k_s is the shear correction factor which needs a detailed elasticity analysis to be determined. We have assumed $k_s = 5/6$. The mass moment of inertia I_i in Eq, (8) are calculated by:

$$[10] \qquad I_i = \int_{-h/2}^{h/2} z^{i-1} \rho(z)\, dz, \qquad i = 1, 2, 3$$

4 SPATIAL SOLUTION

The numerical Galerkin method is adopted here for solving the governing differential equations. Mathematical expressions for boundary conditions considered in this paper are presented here (Reddy 2004, Sarvestani et al. 2011, 2016):

(a) Simply-supported edges at $x = 0$, a; and $y = 0$, b (SSSS):

$$[11a] \qquad u_0 = M_{yy} = \varphi_x = w_0 = N_{yy} = 0 \quad \text{at} \quad y = 0 \quad \text{and} \quad b$$
$$v_0 = M_{xx} = \varphi_y = w_0 = N_{xx} = 0 \quad \text{at} \quad x = 0 \quad \text{and} \quad a$$

(b) Clamped edges at $x = 0$, a; and simply-supported edges at $y = 0$, b (CSCS):

$$[11b] \quad u_0 = v_0 = w_0 = \varphi_x = \varphi_y = 0 \quad \text{at} \quad x = 0 \quad \text{and} \quad a$$

$$u_0 = M_{yy} = \varphi_x = w_0 = N_{yy} = 0 \quad \text{at} \quad y = 0 \quad \text{and} \quad b$$

(c) Clamped edges at $x = 0$, a; and $y = 0$, b (CCCC):

$$[11c] \quad u_0 = v_0 = w_0 = \varphi_x = \varphi_y = 0 \quad \text{at} \quad x = 0 \quad \text{and} \quad a$$

$$u_0 = v_0 = w_0 = \varphi_x = \varphi_y = 0 \quad \text{at} \quad y = 0 \quad \text{and} \quad b$$

(d) Free edges at $x = 0$, a; and simply-supported edges at $y = 0$, b (FSFS):

$$[11d] \quad N_{xx} = N_{xy} = M_{xy} = M_{xx} = Q_x = 0 \quad \text{at} \quad x = 0 \quad \text{and} \quad a$$

$$u_0 = M_{yy} = \varphi_x = w_0 = N_{yy} = 0 \quad \text{at} \quad y = 0 \quad \text{and} \quad b$$

To implement the Galerkin method, the displacement field can be expressed in the following form for arbitrary boundary conditions:

$$[12] \quad u_0(x,y,t) = \sum_{n=1}^{\infty}\sum_{m=1}^{\infty} U_{mn}^0 \Phi_{1m}(x)\Phi_{1n}(y)e^{iwt}, \qquad w_0(x,y,t) = \sum_{n=1}^{\infty}\sum_{m=1}^{\infty} W_{mn}^0 \Phi_{2m}(x)\Phi_{1n}(y)e^{iwt}$$

$$v_0(x,y,t) = \sum_{n=1}^{\infty}\sum_{m=1}^{\infty} V_{mn}^0 \Phi_{2m}(x)\Phi_{2n}(y)e^{iwt}, \qquad \varphi_x(x,y,t) = \sum_{n=1}^{\infty}\sum_{m=1}^{\infty} X_{mn}^0 \Phi_{1m}(x)\Phi_{1n}(y)e^{iwt}$$

$$\varphi_y(x,y,t) = \sum_{n=1}^{\infty}\sum_{m=1}^{\infty} Y_{mn}^0 \Phi_{2m}(x)\Phi_{2n}(y)e^{iwt}$$

where U_{mn}^0, V_{mn}^0, W_{mn}^0, X_{mn}^0, and Y_{mn}^0 are unknown coefficients to be determined. Substituting Eqs. (12) into Eqs. (8) leads to the following matrix form of set of differential equations:

$$[13] \quad \left(\begin{bmatrix} K_{11} & K_{12} & K_{13} & K_{14} & K_{15} \\ K_{21} & K_{22} & K_{23} & K_{24} & K_{25} \\ K_{31} & K_{32} & K_{33} & K_{34} & K_{35} \\ K_{41} & K_{42} & K_{43} & K_{44} & K_{45} \\ K_{51} & K_{52} & K_{53} & K_{54} & K_{55} \end{bmatrix} - \omega^2 \begin{bmatrix} M_{11} & 0 & 0 & M_{14} & 0 \\ 0 & M_{22} & 0 & 0 & M_{25} \\ 0 & 0 & M_{33} & 0 & 0 \\ M_{41} & 0 & 0 & M_{44} & 0 \\ 0 & M_{52} & 0 & 0 & M_{55} \end{bmatrix} \right) \begin{Bmatrix} U_{mn}^0 \\ V_{mn}^0 \\ W_{mn}^0 \\ X_{mn}^0 \\ Y_{mn}^0 \end{Bmatrix} = \begin{Bmatrix} 0 \\ 0 \\ 0 \\ 0 \\ 0 \end{Bmatrix}$$

It should be mentioned that [M] and [K] are symmetric stiffness and mass matrices, respectively. The fundamental frequency of the panels can be obtained by solving the following eigenvalue problem:

$$[14] \quad \left| [K] - \omega^2 [M] \right| = 0$$

where ω is fundamental frequency of the FG panel. The smallest eigenvalue obtained from Eq. (14) is called the fundamental vibration frequency. Admissible trigonometric expansions for different boundary conditions of doubly-curved nano-panels are presented in Table 1, in which the symbols SS, CC, and FF stand for simply-supported, clamped and free edges, respectively.

Table 1: Admissible functions for FG doubly-curved nano-panels for alternative boundary conditions (Reddy 2004).

B.C.	Admissible Functions			
	$\Phi_{1m}(x)$	$\Phi_{2m}(x)$	$\Phi_{1n}(y)$	$\Phi_{2n}(y)$
SSSS*	$\cos(\lambda_m x)$	$\sin(\lambda_m x)$	$\sin(\lambda_n y)$	$\cos(\lambda_n y)$
CSCS*	$\sin(2\lambda_m x)$	$\cos(2\lambda_m x)-1$	$\sin(\lambda_n y)$	$\cos(\lambda_n y)$
CCCC*	$\cos(2\lambda_m x)-1$	$\sin(2\lambda_m x)$	$\sin(2\lambda_n y)$	$\cos(2\lambda_n y)-1$
FSFS**	$\cos(\lambda_m x)+\cosh(\lambda_m x)-\alpha_m(\sin(\lambda_m x)+\sinh(\lambda_m x))$	$\sin(\lambda_m x)+\sinh(\lambda_m x)-\alpha_m(\cos(\lambda_m x)+\cosh(\lambda_m x))$	$\sin(\lambda_n y)$	$\cos(\lambda_n y)$

* For SSSS, CSCS, and CCCC boundary conditions, $\lambda_m = m\pi/a$ and $\lambda_n = n\pi/b$, in which m and n are the half-wave numbers in x and y directions.

** For FSFS boundary condition $\lambda_m = (2m+1)\pi/2a$ and $\lambda_n = n\pi/b$ with $\alpha_1 = 1.0178$, $\alpha_2 = 0.99922$, and $\alpha_m = 1$ $m>2$.

5 HOMOGENIZED PROPERTIES OF FGMS

Since volume fraction is gradually changing through the thickness of the size-dependent doubly-curved FG panels, it is reasonable to assume a representative volume element (RVE) periodically repeated through the planes of the panel each parallel to the x-y plane. While the volume fraction of matrix (V_f) gradually changes through the thickness of panels in the form of a polynomial function, homogenization technique can be used to obtain the effective multiphysical properties for each RVE with specific volume fraction of matrix and inclusion shape. Among alternative methods for homogenization, the standard mechanics homogenization is used here to estimate the mechanical properties of FGMs at each spatial coordinate through the panel (Hassani et al. 1998). In this approach, a portion of the material called as Representative Volume Element (RVE) is chosen and then the standard weak form of the equilibrium equation is solved by applying periodic boundary conditions and independent unit strains on the RVE. Thereafter, the effective mechanical properties of the material can be predicted by volumetric averaging of the calculated stress and strain in the RVE (Akbarzadeh et al. 2016):

$$[15] \qquad \bar{C}_{ijkl} = \frac{1}{V_{RVE}} \int C_{ijmn} M_{mnkl} dV_{RVE}$$

where $\bar{C}_{ijkl}$ is the effective stiffness tensor, V_{RVE} represents the volume of the RVE (replaced by the area A_{RVE} for planar RVEs), C_{ijmn} is the stiffness tensor, and M_{mnkl} stands for the local structural tensor, which relates the average strain $\bar{\varepsilon}_{kl}$ and local or microstructural strain ε_{ij} as $\varepsilon_{ij} = M_{ijkl}\bar{\varepsilon}_{kl}$. To examine the effect of matrix material on the effective properties of the particulate composites and FGMs, three different materials summarized in Table 2 are considered in this paper.

Table 2: Mechanical properties of matrixes and inclusion considered in this study (Doghri et al. 1998).

	Material	Young's modulus (GPa)	Poisson's ratio
Matrix	Epoxy	3.16	0.35
	Aluminum alloy	75	0.30
	Low carbon steel	210	0.30
Inclusion	Silica	73.1	0.18

6 RESULTS AND DISCUSSION

In this section, the vibration responses of size-dependent FG doubly-curved panels are investigated in this section. The size-dependent FG doubly-curved panel can be composed of square or circular silica inclusions with a continuous transition of matrix volume fraction (V_f), made of three different materials, through the panel thickness. The top of the doubly-curved nano-panel is matrix rich ($V_f = 1$), while the bottom side is inclusion rich ($V_f = 0$). Numerical results are presented for FG panels composed of low-carbon steel as a matrix with Silica inclusions of circular topology (unless otherwise specified). Time, moving point load velocity (V) used for forced vibration analysis, and fundamental frequency (ω) are given in the following non-dimensional form:

$$[16] \qquad \bar{t} = \frac{t}{a}\sqrt{\frac{E_m}{\rho_m}}, \qquad \bar{V} = V\sqrt{\frac{E_m}{\rho_m}}, \qquad \bar{\omega} = \omega\frac{a^2}{h}\sqrt{\frac{\rho_m}{E_m}}$$

6.1 Verification studies

In order to validate the accuracy of the developed model and proposed methodology, numerical results are first compared with existing data presented in the literature. As a result, non-dimensional fundamental frequencies obtained by the developed model for simply-supported FG square nano-plates are compared with those of reported in reference (Thai et al. 2013) based on the Mindlin plate theory and modified couple stress theory. Table 3 presents the fundamental frequency of a simply-supported FG square nano-plates with p = 1 for various length-to-thickness ratio (a/h). As seen in Table 3, the maximum difference of 0.4% is found between the results, confirming the accuracy of our developed methodology (Thai et al. 2013).

Table 3: Comparison of non-dimensional fundamental frequency ($\bar{\omega}$) of a simply-supported square FG nano-plate.

a/h	*l/h*	Present	Thai et al. 2013
5	0	4.7865	4.8744
	0.2	5.3062	5.3239
	0.4	6.4105	6.4600
	0.6	7.8895	7.9298

	0.8	9.4602	9.4998
	1	11.0125	11.0451
10	0	5.2235	5.2697
	0.2	5.7145	5.7518
	0.4	6.9187	6.9920
	0.6	8.6098	8.6477
	0.8	10.4264	10.4942
	1	12.3846	12.4128

6.2 Free and forced vibration analysis

In this section, free and forced vibration analyses of size-dependent FG doubly-curved panels are examined. Effects of the thickness-to-length ratio (*h*/*a*), and the curvature-to-length ratio (*R*/*a*) on the non-dimensional fundamental frequency ($\bar{\omega}$) for an FG square nano-plate (ℓ/h = 0.1, and p = 1) considering four different boundary conditions mentioned in Table 1 are presented in Figs. 2a and 2b, respectively. Observing Fig. 2a, increasing value of the thickness-to-length ratio leads to a decrease the fundamental frequency. It is seen from Fig. 2b that as the curvature-to-length ratio increases, the frequency decreases to a constant value, which is different for each boundary conditions. The effects of the curvature-to-length ratio on the frequency are more significant when the doubly-curved nano-panel has the edge conditions of SSSS, or FSFS.

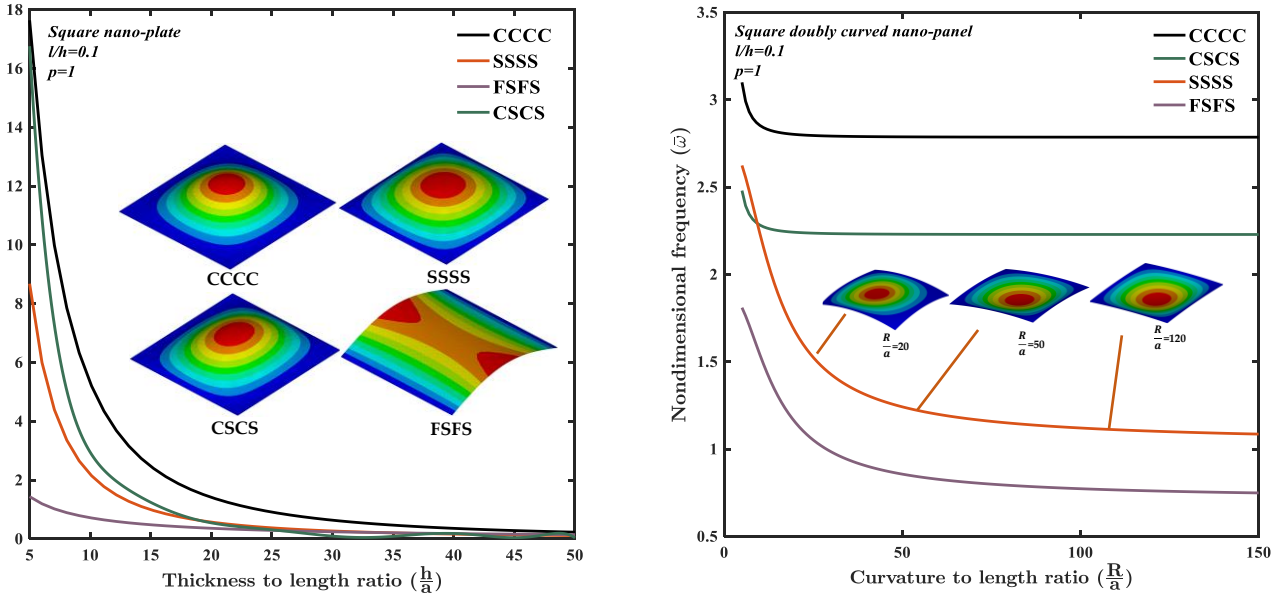

(a) (b)

Figure 2: Effect of (a) thickness-to-length ratio (***h/a***), and (b) curvature-to-length ratio (***R/a***) on the non-dimensional fundamental frequency ($\bar{\boldsymbol{\omega}}$) of an FG square doubly-curved nano-panel.

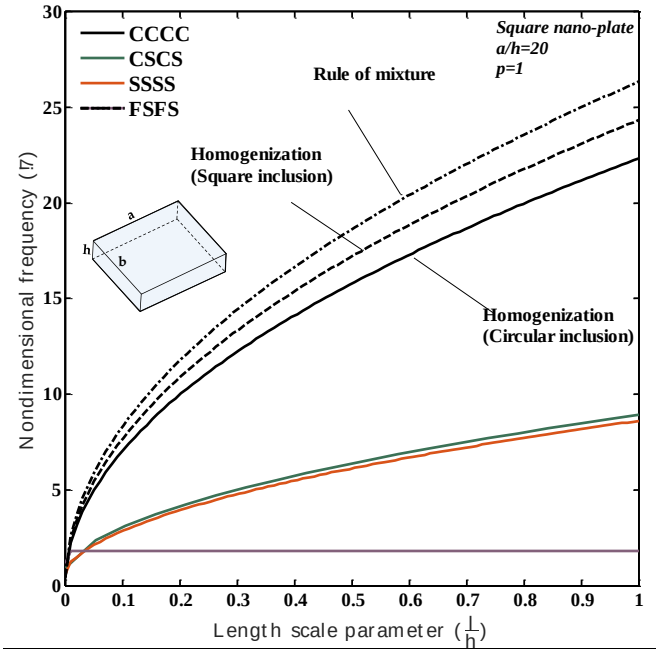

Figure 3: Effect of length scale (***l/h***) on the non-dimensional fundamental frequency ($\bar{\omega}$) of an FG square nano-plate.

Figure 3 demonstrates the effect of non-dimensional length scale (*ℓ/h*) on free vibration behavior of an FG square nano-plate (*a/h* = 20, and *p* = 1) for all four boundary conditions. It is seen that the fundamental frequencies ($\bar{\omega}$) of the nano-plates increase with an increase in the length scale. Moreover, the ratio of the increase in the fundamental frequency varies for different boundary conditions. Figure 4 presents the dynamic response of an FG square nano-plate (*ℓ/h* = 0.1, *p* = 1, and *a/h* = 20). The FG nano-plate is subjected to a moving point load traveling at the middle of nano-plate (*y=b/2*) along the length with non-dimensional velocity $\bar{V}$ = 0.05. Figure 4 shows that the temporal evolution of deflection at the plate midpoint possesses two response domains including forced ($\bar{t} \leq \bar{t}_{exit}$ = 20) and free ($\bar{t}_{exit} \leq \bar{t}$ = 20) vibration parts. A moving transverse point load is applied at the top of the nano-plate and causes the forced vibration up to the exit time of the point load $\bar{t}_{exit}$. Once the moving point load leaves the nano-plate, the FG nano-plate experiences the free-vibration caused by the inertial disturbance of the point load in the force-vibration domain.

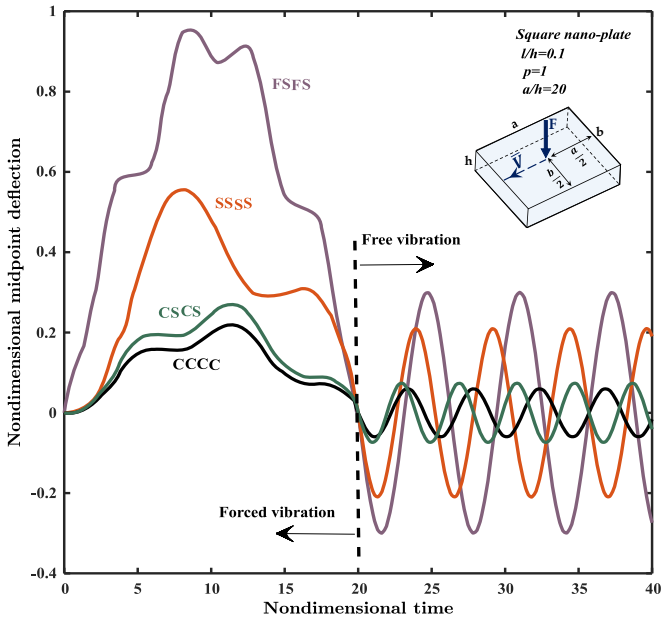

Figure 4: Temporal response of the midpoint deflection of an FG square nano-plate subjected to a moving point load.

7 CONCLUSION

The modified couple stress theory and FSDT are used to investigate the effects of material and geometrical parameters on the free and forced vibration of size-dependent FG doubly-curved panels with considering different sets of boundary conditions. Effective mechanical properties of FG doubly curved panels are estimated using the standard mechanics homogenization technique. The nano-panels considered in this paper are spherical, saddle, cylindrical, and flat panels. The effects of material variation, aspect ratio, curvature, and length scale on the fundamental frequencies of size-dependent FG doubly-curved panels are studied for alternative boundary conditions to provide a robust framework for designing advanced nano/micro scale panels. The major findings of this study can be highlighted as:

- Increasing the length scale causes a higher fundamental frequency for size-dependent FG doubly-curved panels.
- Fundamental frequencies of size-dependent two-phase FG doubly-curved panels with square inclusions are up to 3% higher than those of FG panels are with circular inclusions.

REFERENCES

Akbarzadeh AH, Fu JW, Liu L, Chen ZT, Pasini D. 2016. Electrically conducting sandwich cylinder with a planar lattice core under prescribed eigenstrain and magnetic field. Composite Structures **153**:632-44.

Akbarzadeh AH, Abedini A, Chen ZT, Effect of micromechanical models on structural responses of functionally graded plates. Composite Structures **119**: 598-609.

Asghari M, Rahaeifard M, Kahrobaiyan MH, Ahmadian MT. 2011. The modified couple stress functionally graded Timoshenko beam formulation. Materials & Design **32**(3):1435-43.

Doghri I, Ouaar A. 2003. Homogenization of two-phase elasto-plastic composite materials and structures: study of tangent operators, cyclic plasticity and numerical algorithms. International Journal of Solids and structures **40**(7):1681-712.

Eringen AC. 1972. Nonlocal polar elastic continua. Int. J. Eng. Sci. **10**:1–16.

Hadjesfandiari AR, Dargush GF. 2011. Couple stress theory for solids. International Journal of Solids and Structures **48**(18):2496-510.

Hassani B, Hinton E. 1998. A review of homogenization and topology optimization I-homogenization theory for media with periodic structure. Computers & Structures **69**(6):707-17.

Kiani Y, Akbarzadeh AH, Chen ZT, Eslami MR. 2012. Static and dynamic analysis of an FGM doubly curved panel resting on the Pasternak-type elastic foundation. Composite Structures **94**(8):2474-2484.
Koiter WT. 1964. Couple stresses in the theory of elasticity, I and II. Nederl. Akad. Wetensch. Proc. Ser. B. **67**:17–29.
Kong S, Zhou S, Nie Z, Wang K. 2008. The size-dependent natural frequency of Bernoulli–Euler micro-beams. International Journal of Engineering Science **46**(5):427-37.
Ma, H.M., Gao, X.L., Reddy, J.N. 2008. A microstructure-dependent Timoshenko beam model based on a modified couple stress theory. J. Mech. Phys. Solids **56**:3379–3391.
Mindlin RD, Tiersten H. 1962. Effects of couple-stresses in linear elasticity. Arch. Rat. Mech. Anal.**11**:415–448.
Park SK, Gao XL. 2006. Bernoulli–Euler beam model based on a modified couple stress theory. Journal of Micromechanics and Microengineering **16**(11):2355.
Reddy JN, Berry J. 2012. Nonlinear theories of axisymmetric bending of functionally graded circular plates with modified couple stress. Composite Structures **94**(12):3664-8.
Reddy JN. Mechanics of laminated composite plates and shells: theory and analysis. CRC press; 2004.
Sarvestani HY, Ghayoor H. 2016. Free vibration analysis of curved nanotube structures. International Journal of Non-Linear Mechanics **86**:167-73.
Sarvestani HY, Sarvestani MY. 2011. Interlaminar stress analysis of general composite laminates. International Journal of Mechanical Sciences **53**(11):958-67.
Thai HT, Choi DH. 2013. Size-dependent functionally graded Kirchhoff and Mindlin plate models based on a modified couple stress theory. Composite Structures **95**:142-53.
Tornabene F, Viola E, Fantuzzi N. 2013. General higher-order equivalent single layer theory for free vibrations of doubly-curved laminated composite shells and panels. Composite Structures **104**: 94-117.
Tsiatas GC. 2009. A new Kirchhoff plate model based on a modified couple stress theory. International Journal of Solids and Structures **46**(13):2757-64.
Wang L. 2010. Size-dependent vibration characteristics of fluid-conveying microtubes. Journal of Fluids and Structures **26**(4):675-84.
Yang F, Chong ACM, Lam DCC, Tong P. 2002. Couple stress based strain gradient theory for elasticity. Int. J. Solids Struct **39**:2731–2743.